Analysis of shock response for satellite separation

T. Kitamura[1], K. Yoshida[1], H. Seko[2], Q. Shi[3]
[1] Mitsubishi Electric Corporation, Advanced Technology R&D Center
8-1-1 Tsukaguchi-honmachi, Amagasaki, Hyogo, 661-8661, Japan
e-mail: **Toru.Kitamura@ea.MitsubishiElectric.co.jp**

[2] Mitsubishi Electric Corporation, Kamakura Works
325 Kamimachiya, Kamakura, Kanagawa, 247-8520, Japan

[3] Japan Aerospace Exploration Agency, Environmental Test Technology Center
2-1-1 Senegen, Tsukuba, Ibaraki, 305-8505, Japan

Abstract
When a satellite separates from the rocket in space, large shocks occur in the satellite's body structure. To evaluate the reliability of onboard equipment, the acceleration in the body structure at the time of pyrotechnic operation needs to be predicted at the design stage of the satellite and onboard equipment. We present a method for analyzing separation shock response on satellites. We first made a finite element model on the basis of information on the design of the satellite. We then used static analysis to calculate the force loaded onto the part of the satellite that eventually separates from the body of the rocket by the clamping of the 'V-band clamp'. We then used an input parameter for the force that is released to predict the shock response on the satellite body. Transient response analysis with the mode superposition method was used. By comparing the calculation with the shock test result, we found that the proposed method was effective by considering the panels coupled to the cylinder in addition to the cylinder which was the part of the satellite involved in the separation.

1 Introduction

The body structure of an artificial satellite is subjected to a large shock when the satellite separates from the rocket in space(e.g. [1]-[3]). The most important mechanism for separating the satellite and rocket is a V-band clamp (named for its cross-sectional shape) that provides hold and releasing functions. The satellite and rocket are held together by the V-band clamp, which is fit around the interface between the rocket and satellite. Release is effected by using pyrotechnics to break the V-band clamp. The shock created when the V-band clamp is released propagates to the satellite body structure and creates a load on the payload equipment. The reliability of the equipment with respect to this shock is evaluated with a pre-launch shock test in which pyrotechnics is used to apply a shock to the satellite body structure and the acceleration created in the equipment mounting is measured. If the results of that shock test show that the acceleration exceeds the design specification, re-testing of performance or measures to reduce vibration are required. To evaluate the resistance of the payload equipment to shock and to reduce the costs of anti-vibration measures and retesting, it is important to estimate the acceleration on the satellite body structure caused by the pyrotechnics at the design stage of the satellite body structure and payload equipment development.

Estimating the acceleration of the satellite body structure is currently based on a database of results from previous shock testing, which includes data such as attenuation curves that have the acceleration near the source of the shock and the distance from the source as parameters and attenuation at the mechanical fastening. However, the shock test databases in Japan have only a small number of samples, and error in estimations based on such empirical rules is a major problem. Because satellites produced in Japan differ in specifications from the satellites of other countries, there is a tendency for the results of shock testing to

also differ. The shock test data for non-Japanese satellites therefore cannot be used without modification. To improve the reliability of the payload equipment, it is therefore necessary to estimate the response of the satellite body structure to the shock from the action of the pyrotechnics at the stage of satellite and payload equipment design. Establishing a method for such estimation, can contribute greatly to shortening the development design and testing period and to reducing the cost of development design, test and anti-vibration measures.

A number of analytical methods based on fundamental experiments concerning estimation of shock response at the time of satellite separation are underway in Japan. One example is a method in which the separation structure on the satellite side is modeled as an axially symmetrical cylindrical shell and the V-band clamp is modeled as a multiple-degree-of-freedom vibration system with mass elements to estimate the acceleration of the satellite body structure generated when the separation mechanism operates [4]. That modeling method is useful for structures that have axial symmetry and the distance from the plane of satellite separation and the constrained part of the cylindrical shell is sufficiently long. For separation structures in which the distance between the plane of satellite separation and the cylindrical shell constraint is short, however, the effects of the boundary conditions of the cylindrical shell are large and determining those boundary conditions is difficult. Estimation accuracy is therefore a problem. Research in which the separation structure on the satellite side is taken to be a torus and modeled as a vibration system that has single-degree-of-freedom to estimate the acceleration also shows that this approach is useful when the expansion and contraction primary mode response of the torus is dominant [5]-[7]. However, it cannot be applied when high-frequency components that are equal to or greater than the secondary mode expansion and contraction are not negligible or when the torus bending modes of lower frequency than the expansion and contraction mode cannot be neglected. Furthermore, the main problem with these estimation methods is the modeling of the separation structure. For that reason, it has not been possible to quantitatively evaluate the excitation load on the satellite body structure at the time of separation without determining the compressive force generated in the separation structure on satellite by the fastening of the V-band clamp at the time the V-band clamp is released.

As a solution to the problems described above, we report an investigation of using a terrestrial testing model of the satellite for accurate determination of the excitation force when the V-band clamp is released and a precise modeling method to raise the accuracy of estimating the acceleration of the satellite body structure that arises at the time of separation of satellite and rocket.

2 Test sample and separation structure

The test sample was a terrestrial testing model of a satellite that has been launched successfully. We considered the satellite body with the antennae and solar cell paddles removed. An overview of the satellite body is shown in figure 1. Schematic views of the fastening between the satellite and the rocket are shown in figure 2. figure 2 shows that the separation structure on the satellite side (the lower part of the central cylinder) and the separation structure on the rocket side are held together by the fastening of V-band clamps. The hold-down/release mechanism of the V-band clamps is shown in figure 3. The configuration is such that the fastening is released by using pyrotechnics to sever the fastening bolts of the V-band clamps, to separate the satellite and the rocket. The relationship between the satellite coordinates (XYZ) shown in figure 1 and the locations where the V-band clamps act is shown in figure 4. As shown in figure 4, the V-band clamps are released from two positions: regions I and III. The regions I and III from which the V-band clamps are released are offset by 22.5 degrees from the X-axis of the satellite coordinates. With this satellite, the distance between the satellite separation plane and the body panel attachments is short, and an anti-earth panel is attached at approximately 100 mm away. figure 5 shows the situation in which the separation structures on the satellite body and rocket side are fastened together with a V-band clamp and a pyrotechnic is installed.

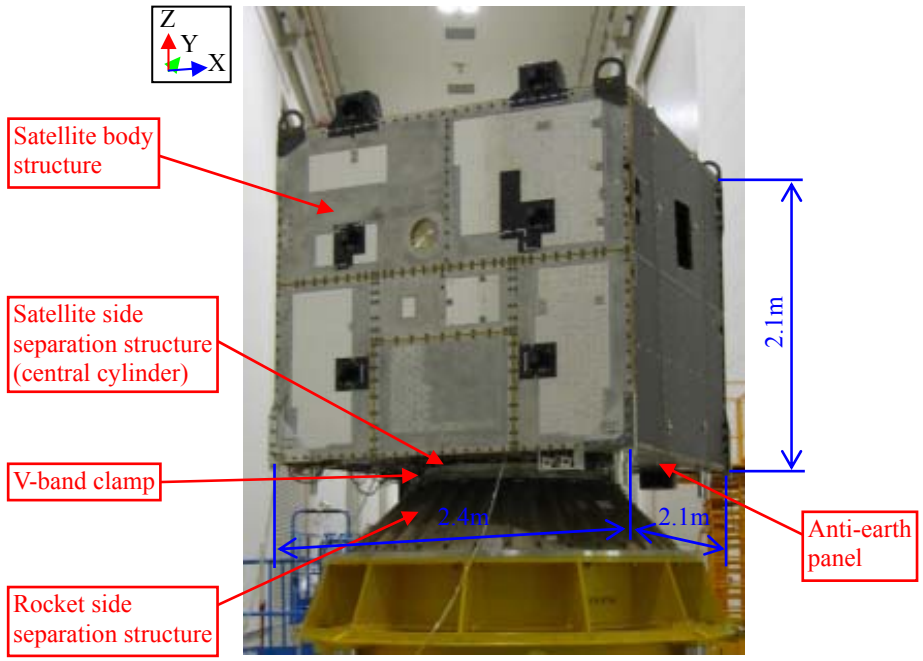

Figure 1: Overview of test specimen

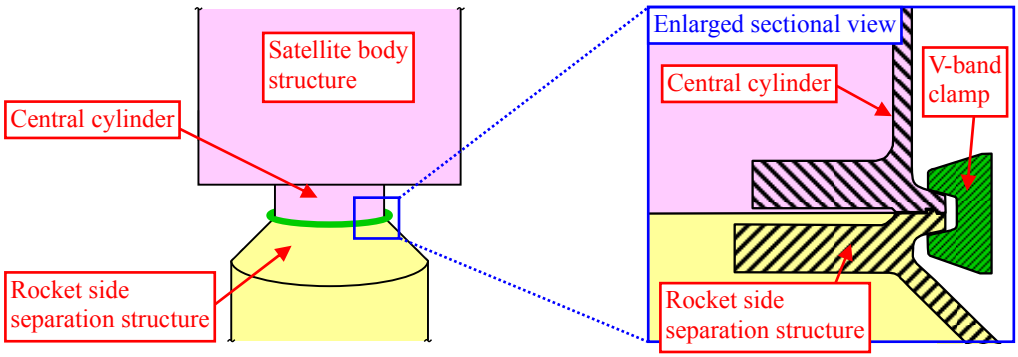

Figure 2: Schematic view of separation part of satellite and rocket

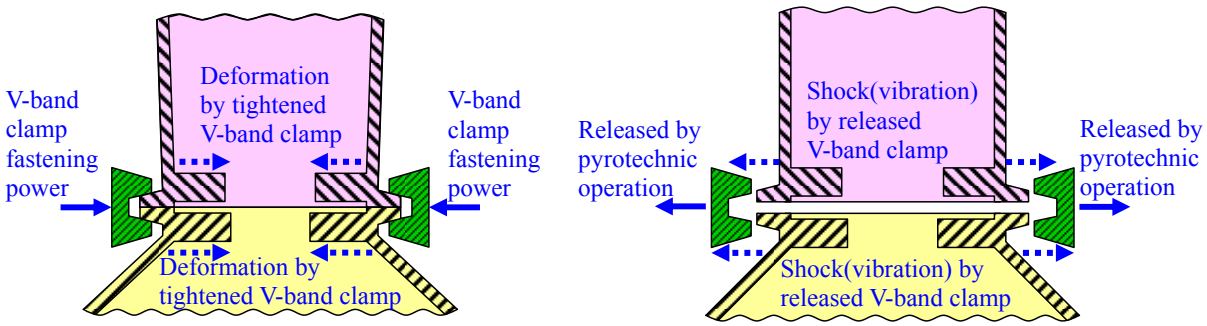

(a) Holding down by V-band clamps (b) Released V-band clamp

Figure 3: Hold-down and release mechanism of V-band clamp

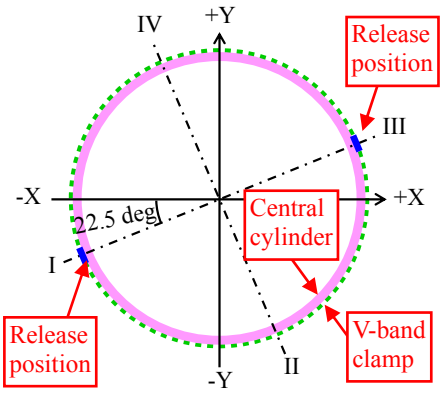

Figure 4: Relations of the satellite coordinate and position of V-band clamp when released

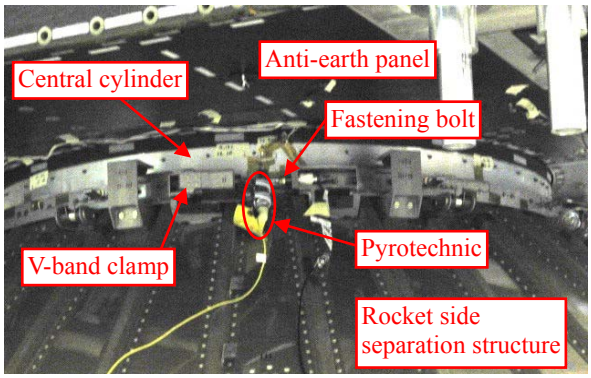

Figure 5: Overview of area around V-band clamp at pyrotechnic implementation

3 Vibration response analysis

There are three steps in the proposed procedure for estimating the accelerations that are generated on the satellite body when the separation structures of the satellite and the rocket are released. In the first step, we create a finite element model based on design information (dimensions and material properties) of the satellite body, and verify the vibrational validity of the finite element model by experimental modal analysis. In the second step, we compute the forces exerted on the central cylinder (called the V-band clamp fastening power in the rest of this paper) by static analysis. We identify the force at which the V-band clamp fastening power is released in a step-wise function to be the excitation force exerted on the satellite body. In the third step, we use the thus-identified excitation force as an input parameter to compute a time history response by transient response analysis implemented by a mode superimposition method, and compute the vibrational responses generated in the satellite body.

There has been some research into the estimation of the V-band clamp fastening power for the second step, such as estimation of the forces generated in the V-band clamp from the shape of the V-band clamp[8], estimation of the V-band clamp fastening power from the shape of the V-band clamp and the tension fastened by the V-band clamp[4], and estimation of the displacement of the central cylinder[5], but these have not been able to confirm the deformations of the central cylinder generated by the fastening of the V-band clamps. To solve this problem, this paper computes the V-band clamp fastening power from static analysis using measured values of strain generated in the central cylinder when it is fastened by the V-band clamps, and identifies the excitation forces exerted on the satellite body.

3.1 Creation of finite element model

3.1.1 Modeling

To investigate the vibrations generated in the central cylinder shown in figure 1, we created two finite element models: (1) a modeling of just the central cylinder (called the cylinder model below), and (2) a modeling of an assembly constructed from the central cylinder and web panels for increasing the rigidity of the central cylinder and the anti-earth panel on the base surface of the satellite body, as shown in figure 1, (called the assembly model below). An overview of these finite element models is shown in figure 6. With the cylinder model (1), we verify the computational accuracy when it has been modeled simply in a cylindrical shell. With the assembly model (2), we take into account the effects of the central cylinder and coupling panels and the asymmetric properties of the structure.

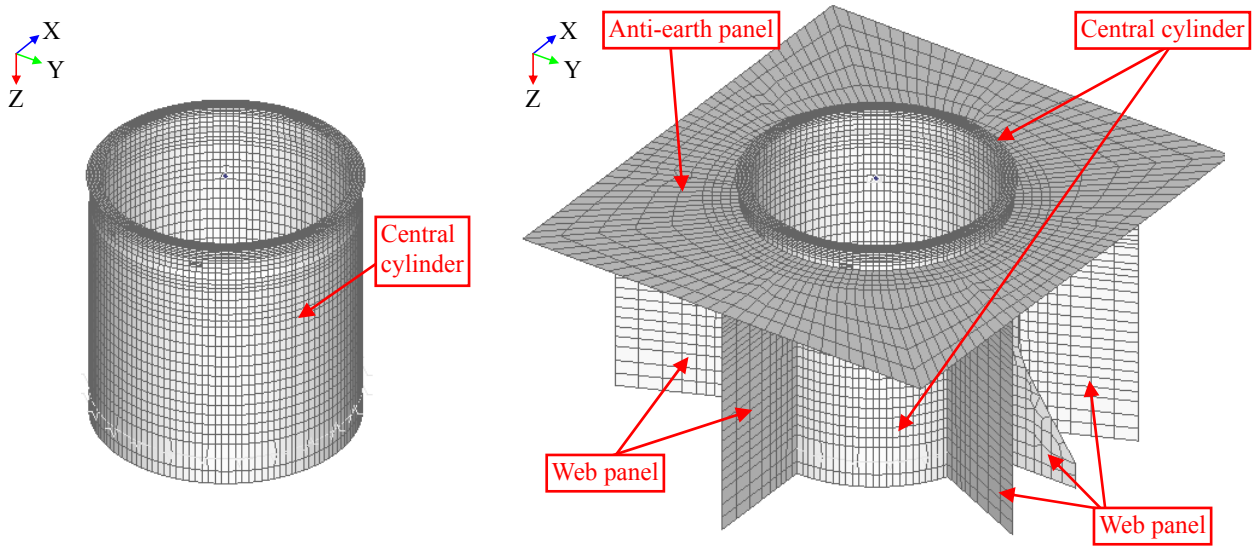

(1) Cylinder model (2) Assembly model

Figure 6: Overview of finite element model

3.1.2 Verification of validity of finite element models

(a) Numerical modal analysis

The results of modal analysis calculated by ordinary structural analysis software, MSC Nastran Version 2010, are shown in Table 1. Table 1 shows the part of the central cylinder below the anti-earth panel, in order to make it easier to comprehend the vibration mode shapes of the parts in the vicinity of the satellite-side separation plane. From the left-hand column of Table 1, we can confirm that the cylinder model (1) exhibited a circular bending mode with two diametric nodes at 159 Hz, a circular bending mode with three diametric nodes at 240 Hz, a circular bending mode with four diametric nodes at 520 Hz, a circular bending mode with five diametric nodes at 965 Hz, and a primary circular expansion/contraction mode at 1481 Hz. From the center column of Table 1, we can confirm that the assembly model (2) exhibited a circular bending mode with two misshapen diametric nodes at 128 Hz, a circular bending mode with three diametric nodes at 417 Hz, a circular bending mode with four diametric nodes at 658 Hz, a circular bending mode with five diametric nodes at 958 Hz, and a primary circular expansion/contraction mode at 1499 Hz.

(b) Experimental modal analysis

We performed hammering test with the satellite body suspended, without the rocket-side separation structure and V-band clamps fastened to the satellite body. To simplify the validity verification of the finite element models, we set the constraint conditions of the V-band clamp fastener parts to be free. In order to confirm the circular vibration mode shapes of the central cylinder, we measured on the central cylinder at a distance of 5 mm from the satellite separation plane. The results of the experimental modal analysis are shown in the right-hand column of Table 1. We were able to confirm a shape in which a circular bending mode with two diametric nodes was misshapen at 249 Hz, a circular bending mode with three diametric nodes at 360 Hz, a circular bending mode with four diametric nodes at 570 Hz, and a circular bending mode with five diametric nodes at 882 Hz. We also confirmed a circular expansion/contraction mode at 1602 Hz. For modes of higher orders than these circular bending and circular expansion/contraction modes, there were too few measurement points so we were unable to clearly determine such deformation modes.

The vibration mode shapes generally matched for the numerical modal analysis results and experimental modal analysis results of both models. It should be noted that the vibration mode shapes of the assembly model (2) in the circular bending modes with two and three diametric nodes deformed close to practice. The differences in resonant frequency were large for the circular bending modes with two and three

diametric nodes, but were within 15% for the circular bending modes with four or more diametric nodes. In research by Iwasa, et al., the difference in resonant frequency for the primary circular expansion/contraction mode, which was the most dominant vibration mode with respect to vibration of the central cylinder at V-band clamp release, was within 7%[5]-[7].

(a) Numerical modal analysis		(b) Experimental modal analysis
(1) Central cylinder model	(2) Assembly model	
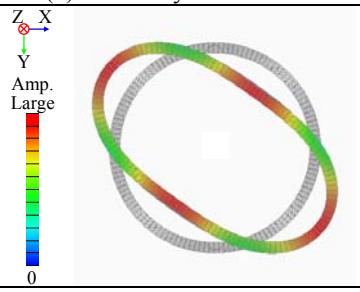	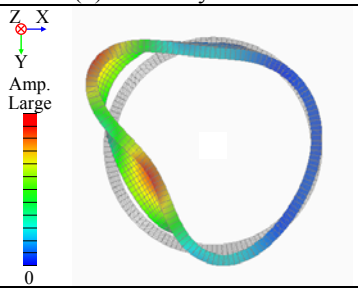	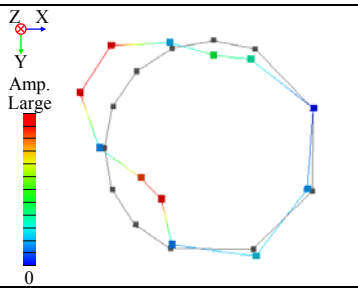
159 Hz	128 Hz	249 Hz
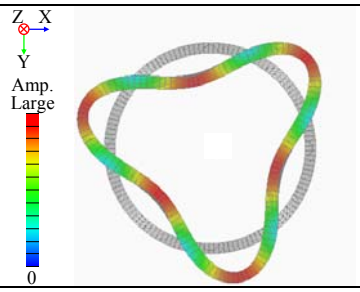	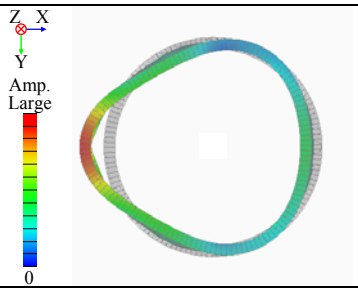	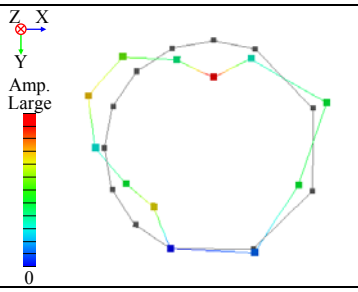
240 Hz	417 Hz	360 Hz
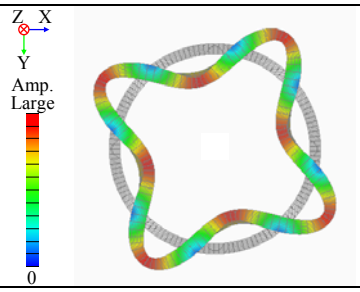	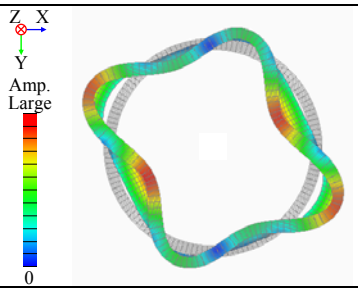	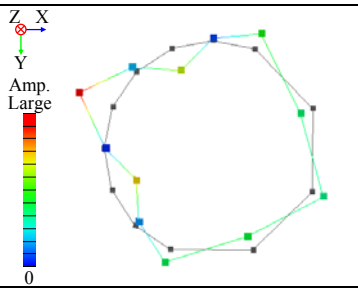
520 Hz	658 Hz	570 Hz
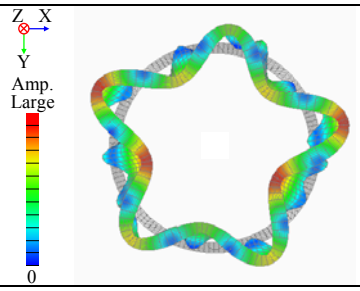	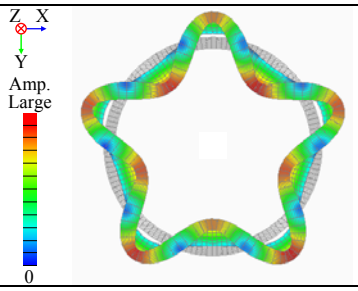	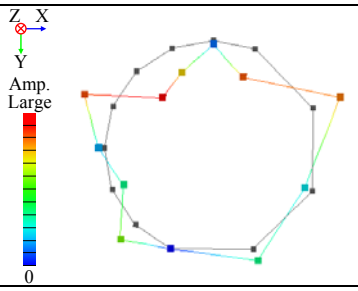
965 Hz	958 Hz	882 Hz
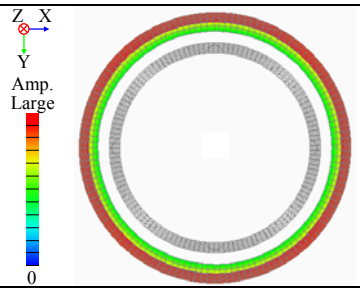	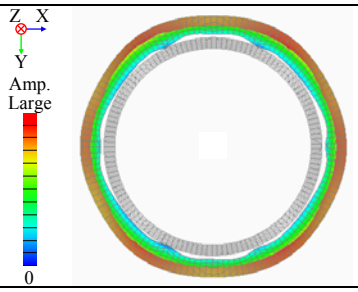	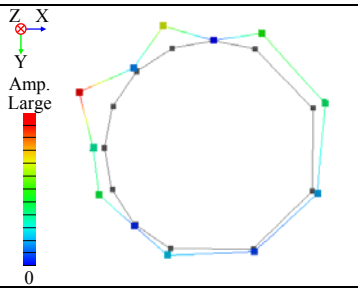
1481 Hz	1499 Hz	1602 Hz

Table 1: Modal characteristics of satellite side separation part

3.2 Estimation of V-band clamp fastening power

3.2.1 Strain measurements

We measured strain in the circumferential direction of the central cylinder, at a distance of 20 mm from the satellite separation plane. The V-band clamps fasten at two locations: regions I and III. During the fastening work, we insert a load cell at each of the two locations of regions I and III and fasten the V-band clamps in such a manner that they act with equal tension. In the fastening of V-band clamps of satellite flight products as well, load cells are inserted and the tensions of the fastening bolts are supervised. The relationship between V-band clamp tension and strain in the circumferential direction of the central cylinder is shown in figure 7. From figure 7, we confirmed a proportional relationship between the V-band clamp tension and strain in the circumferential direction of the central cylinder Since the V-band clamps are fastened at the two locations of regions I and III, the strain at regions I and III of the central cylinder was large. The strain in the circumferential direction of the central cylinder when the V-band clamp fastening power was approximately 18kN was an average of approximately -165 μST (the negative value shows it is in compression) at the two locations of regions I and III and an average of approximately -105 μST at the two locations of regions II and IV, in a ratio of 1:0.64. From this, we can assume that the central cylinder is deformed by the V-band clamp fastenings into a shape that is close to elliptical.

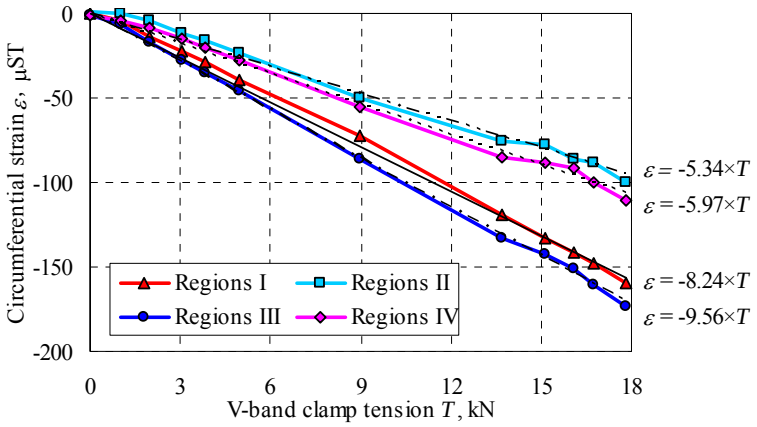

Figure 7: Relations of tension in V-band clamp and circumferential strain of central cylinder

3.2.2 Estimation of V-band clamp fastening power

Using the measured values of strain, we attempted to calculate the V-band clamp fastening power that forms an input condition to the numerical analysis model. In static analysis by the finite element method, enforced displacements with an elliptical distribution were exerted on nodes of the central cylinder that correspond to the V-band clamp contact areas towards an origin in the radial direction, which is the direction in which the central cylinder contracts. The load nodes for the enforced displacements are shown in figure 8. These enforced displacements are determined to optimize the amount of enforced displacement of each node in the numerical analysis to ensure that the values of strain in the circumferential direction of the central cylinder are -165 μST at locations corresponding to regions I and III and -105 μST at locations corresponding to regions II and IV. We also calculate the reactive force that is generated in the central cylinder during this process. Next, we applied a force that is equivalent to the computed node reactive force to the same nodes as those that were subjected to the enforced displacement, without exerting any enforced displacement, and confirmed that values of strain in the circumferential direction were approximately -165 μST for regions I and III and approximately -105 μST for regions II and IV. The thus-exerted force was taken to be the V-band clamp fastening power.

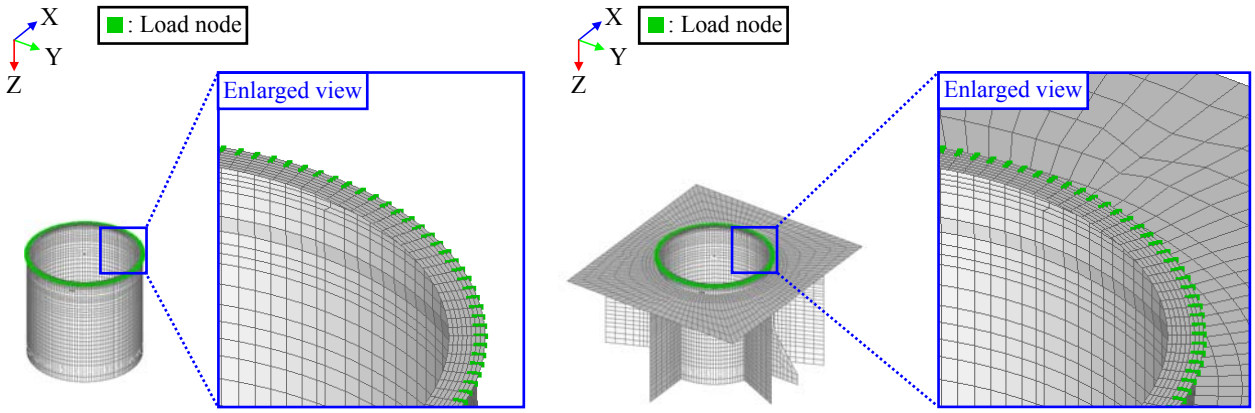

(1)Cylinder model (2)Assembly model

Figure 8: Enforced displacement load nodes

3.3 Simulation and results of shock test

We use a shock response spectrum (SRS) in evaluating accelerations due to the shock phenomenon. When using an acceleration $\ddot{y}$ based on a single-degree-of-freedom vibration system constructed from a mass *m*, a spring constant *k*, and a viscous damping constant *c*, as shown in figure 9, the SRS gives the maximum amplitude of the acceleration $\ddot{x}$ of the mass m in a single-degree-of-freedom vibration system with natural frequency f_n.

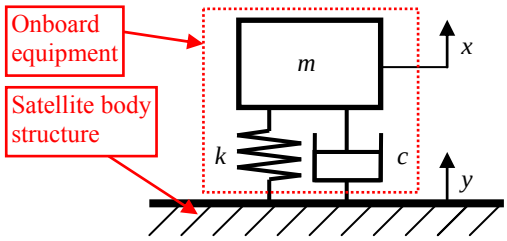

Figure 9: Single-degree-of-freedom vibration system

The equation of motion of the vibration model of figure 9 is as follows:

$$m\ddot{x} + c\dot{x} + kx = c\dot{y} + ky \tag{1}$$

If we assume the natural angular frequency $\omega_n = \sqrt{k/m}$ and damping ratio $\zeta = c/\sqrt{mk}$, this equation can be converted as follows:

$$\ddot{x} + 2\zeta\omega_n\dot{x} + \omega_n{}^2 x = 2\zeta\omega_n\dot{y} + \omega_n{}^2 y \tag{2}$$

The acceleration $\ddot{x}$ of the mass m can be expressed as follows, using the Laplace operator *s*:

$$\ddot{x} = \ddot{y}\left(2\zeta\omega_n s + \omega_n{}^2\right)/\left(s^2 + 2\zeta\omega_n s + \omega_n{}^2\right) \tag{3}$$

We plot the maximum value of equation (3) with respect to the natural frequency f_n of the single-degree-of-freedom vibration system to express the SRS characteristic.

When evaluating shock on the onboard equipment of the satellite, we calculate the SRS on the basis that each piece of onboard equipment is a single-degree-of-freedom vibration system and the satellite body panels to which the onboard equipment is attached act as foundations. Since it is possible to calculate the maximum accelerations at natural values of the single-degree-of-freedom vibration systems when given a

time-history waveform of the fundamental accelerations, SRS is generally used in evaluating the shock phenomenon on satellites[1]-[7].

We identified the force at which the estimated V-band clamp fastening power is released in a step-wise manner to be the excitation force exerted on the satellite body, input that excitation force to the central cylinder, performed a transient response analysis by a mode superimposition method, and calculated the time-history response. We assumed that the damping ratio of the satellite body was 5%. The vibration modes that we considered in the response calculation were all the modes up to 15000 Hz, which were 3656 for the cylinder model (1) and 8059 for the assembly model (2). The numbers of modes at 4000 Hz and below are 1626 for the cylinder model (1) and 3115 for the assembly model (2). Note that these numbers of modes also include out-of-plane vibration modes and local vibration modes of the reinforcing panels, which contribute little to satellite separation. In order to compare the numerical analysis results, we also performed shock experiments using pyrotechnics. Since the onboard equipment is mounted at a distance from the anti-earth panel attachment parts (approximately 100 mm in this satellite model), the points for the evaluation that are necessary for the shock-resistant design of onboard equipment are at three locations: 60 mm from the satellite separation plane directly in front of the anti-earth panel attachment part, and 300 mm and 400 mm from the anti-earth panel attachment parts.

The results of the simulation and shock experiments are shown in figure 10. We calculated the SRS assuming a damping ratio ζ of 5%, from the time-history waveforms of accelerations that were calculated or measured. From figure 10, we see that the acceleration levels with the shock experiments were greatest in the vicinity of 1600 Hz. The experimental modal analysis results of Table 1 enabled us to confirm that the circular expansion/contraction mode of the satellite-side separation structure is prominent with separation shock of the V-band clamp hold/release structure, from the fact that the primary circular expansion/contraction mode is at 1602 Hz. The numerical analysis results show that with the cylinder model (1), vibration levels were large at a peak of approximately 160 Hz and on to the vicinity of 300-400 Hz at all evaluation points, diverging by approximately 30% from the shock experiment results. This is due to excitation of the circular bending mode with two diametric nodes. The error in estimating accelerations in the low frequency bands has a large effect when converting into vibration velocity or displacement, making it difficult to produce a shock-resistant design. When we used the estimation results of this research to create a shock-resistant design, we had no option but to over-design in comparison with the real structure, which was not feasible. With the assembly model (2), the estimation errors were within +10 dB (≈ 3.2 times) or -5 dB (≈ 0.56 times) at maximum, which matched the shock experiment results well. Iwase, et al., have laid out a guideline of +5 dB for the estimated value when prescribing the SRS spec for satellite separation with an approved experiment level of P99/90 (the level that includes 99% of the total, with 90% confidence)[6]. The estimation results of this method are within 5 dB on the negative side of the experimental results, so are said to be sufficiently useful in practice. Because the vibration levels at 400 Hz and below are low in comparison with the cylinder model (1), the circular bending modes of the satellite-side separation structure and the out-of-plane deformation modes of the central cylinder are restrained by the anti-earth panel and web panels, so the modeling can be said to be close to that of the actual structure. When panels are connected to the central cylinder, increasing the rigidity of the central cylinder in the out-of-plane direction, the modeling of just the central cylinder is insufficient, and it became clear that we must study an assembly model that includes even circumferential members. From the above, we have confirmed the validity of this method of estimating the accelerations that are generated on the satellite body during release of the separation structures of the satellite and rocket, by using the assembly model (2) and inputting the V-band clamp fastening power estimated from measured values of strain to the central cylinder by transient response analysis using a mode superimposition method. This has made it possible to estimate accelerations on the satellite body, even when there are structural members such as satellite body panels located close to the satellite separation plane or when there is an asymmetric configuration, in addition to the central cylinder structure to which conventional methods can be applied[4]-[7].

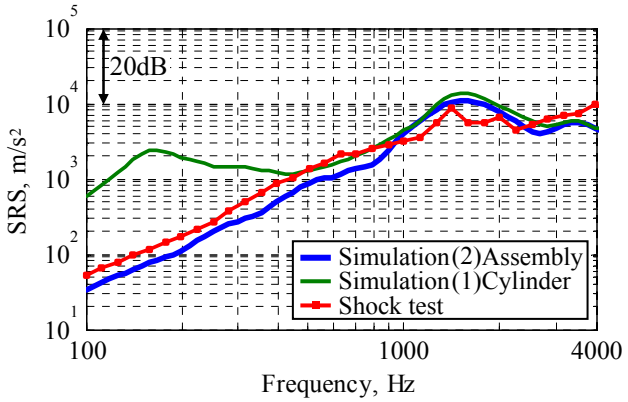

(a) Distance from satellite separation plane: 60 mm

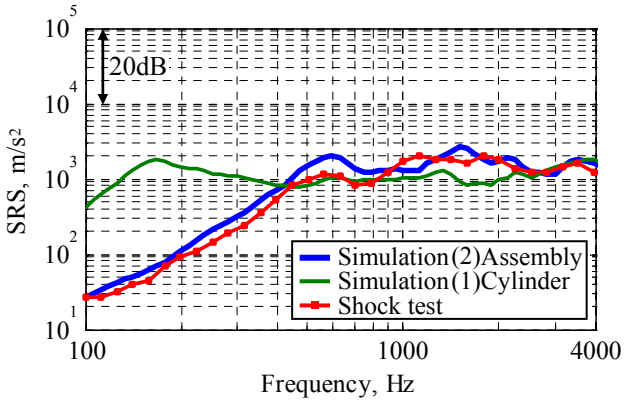

(b) Distance from satellite separation plane: 300 mm

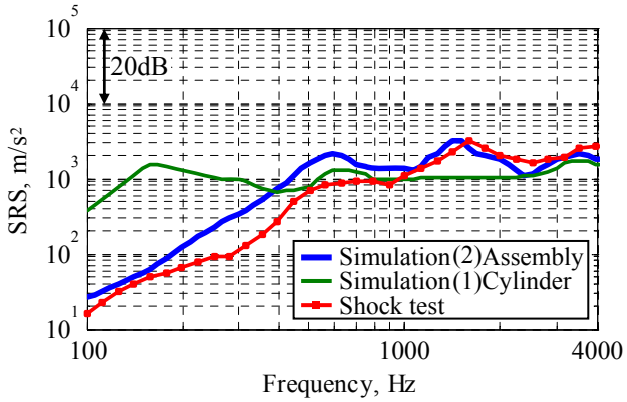

(c) Distance from satellite separation plane: 400 mm

Figure 10: Simulation and test result

4 Conclusion

We have proposed a method of estimating accelerations of a central cylinder as a method of estimating accelerations on a satellite body that are generated during the release of the separation structures of the satellite and the rocket, and have verified it with an actual satellite. The procedure is as follows:

(1) Measure the distribution of strain in the circumferential direction of the central cylinder when fastened by V-band clamps.

(2) Use static analysis to calculate central cylinder displacements and node reactive forces due to the above strain distribution.

(3) Input these node reactive forces to the central cylinder, on the assumption that node reactive forces are released in a step-wise manner, and calculate the accelerations of each part of the central cylinder by transient response analysis using a mode superimposition method.

In step (1) of the above procedure, we found that the central cylinder deformed in an elliptical shape, and the magnitude of the resultant strains were proportional to the tensions of the V-band clamps. If we can understand the tensions of the V-band clamps for other satellites too, it would therefore be possible in the future to make a string of estimations at the design stage before the actual structure is fabricated, from estimations of the distribution of strain in the circumferential direction, without measuring those strains.

In the modeling of step (3) of the above procedure, the results of calculating the responses of two types of model, one of the central cylinder alone and one that considers panels connected to the central cylinder, showed that the estimation accuracy of the second model was greater. The increase in calculation errors of

the first model was because it was not possible to consider that the responses due to the rigidity of each connected panel in the low frequency bands were small.

In the future, we intend to investigate methods of evaluating the shock response of equipment mounted on the satellite body from the shock response of the central cylinder, with the goal of shock design for the entire satellite body.

References

[1] National Aeronautics and Space Administration, *Pyroshock Test Criteria*, National Aeronautics and Space Administration (1999).

[2] National Aeronautics and Space Administration, *Dynamic Environmental Criteria*, National Aeronautics and Space Administration (2001).

[3] T. Kitamura, H. Seko, Q. Shi, K. Nagahama, T. Iwasa, *Shock Data Acquisition and Evaluation of Hold-down and Release Mechanism for Spacecraft*, *Proceedings of The 53rd Symposium on Space Science and Technology, 2001 September 9-11,* The Kyoto (2001), pp. 540-544.

[4] S. Takeuchi, J. Onoda, *Estimation of Separation Shock of the Marman Clamp System by Using a Simple Band-Mass Model*, Transactions of the Japan Society for Aeronautical and Space Sciences, Vol. 45, No. 147, The Japan Society for Aeronautical and Space Sciences (2002), pp. 53-60.

[5] T. Iwasa, Q. Shi, *Simplified Estimating Method for Shock Response Spectrum Envelope of V-Band Clamp Separation Shock*, Journal of Space Engineering, Vol. 1, No. 1, The Japan Society of Mechanical Engineers (2008), pp. 46-57.

[6] T. Iwasa, Q. Shi, *Simplified Analysis Method for Pyroshock Responses Near the Pyroshock Source Induced by V-band Clamp Separation Devices*, Transactions of the Japan Society of Mechanical Engineers Series C, Vol. 74, No. 738, The Japan Society of Mechanical Engineers (2008), pp. 309-317.

[7] T. Iwasa, Q. SHI, *Calculation Method for Flight Limit Load of V-band Clamp Separation Shock*, Journal of Space Engineering, Vol. 3, No. 1, The Japan Society of Mechanical Engineers (2010), pp. 15-23.

[8] K. Shoghi, S.M. Barrans, H.V. Rao, *Stress in V-Section Band Clamps*, Proceedings of the Institute of Mechanical Engineering Part C, Journal of Mechanical Engineering Science, Vol. 218, No. 3 (2004), pp. 251-261.